Article

SCIENCE PROGRESS

Science Progress
2020, Vol. 103(1) 1–17

DOI: 10.1177/0036850419877762
journals.sagepub.com/home/sci
SAGE

Research on braking energy recovery strategy of electric vehicle based on ECE regulation and I curve

Shengqin Li, Bo Yu and Xinyuan Feng
School of Traffic and Transportation, Northeast Forest University, Harbin, China

Abstract

Electric vehicles can convert the kinetic energy of the vehicle into electric energy for recycling. A reasonable braking force distribution strategy is the key to ensure braking stability and the energy recovery rate. For an electric vehicle, based on the ECE regulation curve and ideal braking force distribution (I curve), the braking force distribution strategy of the front and rear axles is designed to study the braking energy recovery control strategy. The fuzzy control method is adopted while the charging power limit of the battery is considered to correct the regenerative braking torque of the motor, the ratio of the regenerative braking force of the motor to the front axle braking force is designed according to different braking strengths, then the braking force distribution and braking energy recovery control strategies for regenerative braking and friction braking are developed. The simulation model of combined vehicle and energy recovery control strategy is established by Simulink and Cruise software. The braking energy recovery control strategy of this article is verified under different braking conditions and New European Driving Cycle conditions. The results show that the control strategy proposed in this article meets the requirements of braking stability. Under the condition of initial state of charge of 75%, the variation of state of charge of braking control strategy in this article is reduced by 8.22%, and the state of charge of braking strategy based on I curve reduces by 9.12%. The braking force distribution curves of the front and rear axle are in line with the braking characteristics, can effectively recover the braking energy, and improve the battery state of charge. Taking the using range of 95%–5% of battery state of charge as calculation target, the cruising range of vehicle with braking control strategy of this article increases to 136.64 km, which showed that the braking control strategy in this article could increase the cruising range of the electric vehicle.

Keywords

Braking energy recovery, fuzzy control, I curve, ECE regulation, co-simulation

Corresponding author:
Bo Yo, School of Traffic and Transportation, Northeast Forest University, 26 Hexing Road, Xiangfang District, Harbin 150040, Heilongjiang, China.
Email: 1091589007@qq.com

Introduction

At present, in the boom of the promotion of new energy vehicles, electric vehicles have attracted much attention due to their advantages in emissions, structure, and technology.[1] However, the problem of the cruising range of electric vehicle has not been effectively solved, and it has become an obstacle to market promotion.[2–4] The electric vehicle drives the wheels by the motor, and at the same time, it can be turned into a generator to take part in braking when the vehicle is braking. It relies on the transmission system to provide the resistance which is needed for the deceleration of the vehicle and converts the kinetic energy of the vehicle into electric energy to be stored in the energy storage components.[5–7] The energy recycling during the braking process is very significant, which can improve the energy utilization efficiency of the vehicle and increase the cruising range.[8,9]

The braking system of electric vehicle consists of a conventional friction braking system and a regenerative braking system of the motor. The main research content of the braking energy recovery strategy is how to distribute the friction braking force of the front and rear axle and the regenerative braking force of the motor. The braking energy has been recovered as much as possible, ensuring the stable braking performance.[10–12] Montazeri-Gh and Mahmoodi-K[13] proposed an optimal energy management system for hybrid electric vehicle (HEV) based on genetic algorithm. The effects of batteries in initial state of charge (SOC) and hybridization factor are investigated on HEV performance to evaluate fuel consumption and emissions. The result showed that fuel consumption average reduction of about 14% is obtained for optimal configuration data in contrast to default configuration. Also, results indicate that proposed controller has reduced emission of about 10% in various traffic conditions. For the two different optimization objectives of braking stability and braking energy feedback efficiency, Gao and Ehsani[14] designed two braking energy distribution strategies for recovering the braking forces of the front and rear wheels based on neural network, and evaluated the energy recovery efficiency of the control strategy proposed. Gao et al.[15] divided the braking mode by vehicle speed and braking strength, proposed a wheel-cylinder pressure control algorithm of the feedforward plus the three closed-loop feedback based on the electric servo system, and coordinated the distribution of electro-hydraulic braking force; the simulation and vehicle platform experiments show the effectiveness of its pressure control algorithm and braking energy recovery strategy. Hu et al.[16] analyzed the mode-shift process from single motor to torque coupling and the jerk value and kinetics relationship of the torque coupling process and signal motor process based on the analysis of the structure. The simulation result shows that the mode-shift process from single motor to torque coupling limited jerk value less than $2.5\,m/s^3$, without a dynamic power interruption. Based on the curve of ideal braking force distribution, Chen et al.[17] used the fuzzy control algorithm to distribute the mechanical braking force and braking force of the motor, and then to exert the regenerative braking characteristics of the motor as much as possible, but did not consider the limitation of the charging and discharging power of battery. Meng[18] designed a regenerative braking control

strategy based on fuzzy control, which could meet the requirements of the braking regulations and recover the braking energy as much as possible. Coordination of the regenerative braking control strategy designing the fuzzy controller, which input is speed, battery SOC and braking strength, and the output is braking force distribution coefficient of the before and after axle and the braking force distribution coefficient of the motor braking force and the mechanical braking force.

In this article, a braking force distribution and braking energy recovery strategies for regenerative braking and friction braking was designed for an FF (Front-engine, front-wheel-drive layout) electric vehicle based on the ideal braking force distribution curve of the vehicle, combining the I curve and *f* line groups, and taking into account the limitations of the Economic Commission for Europe (ECE) regulations. The co-simulation model was established in Simulink and Cruise, and the effectiveness of the control strategy is verified under different braking strength conditions and New European Driving Cycle (NEDC) conditions. Compared with the braking strategy-based I curve, the control strategy proposed in this article could increase the cruising range of vehicles and increase the recovery braking energy.

Force analysis during braking

Braking strength

Braking force distribution strategy for electric vehicles should be designed based on brake safety. Considering the braking safety with each braking strength, the following requirements should be met.

Ideal braking force distribution curve. There are three cases of the lock order of the front and rear axle in the braking process of the vehicle. When braking, if the front and rear axle are simultaneously locked and dragged, the relationship between the front and rear braking forces is called the ideal braking force distribution curve, that is, the I curve. The distribution of the braking force of the vehicle according to the I curve can ensure that the front and rear wheels are locked at the same time on any adhesion coefficient road surface, and the ground attachment conditions are well utilized. At this time, the front and rear axle braking forces satisfy the following relationship

$$F_{br} = \frac{1}{2}\left[\frac{G}{h}\sqrt{b^2 + \frac{4hL}{G}F_{bf}} - \left(\frac{Gb}{h} + 2F_{bf}\right)\right] \tag{1}$$

where F_{bf} is the ground braking force of the front axle (N); F_{br} is the ground braking force of the rear axle (N); G is the vehicle gravity (kg); b is the distance from the center of the mass to the center of the rear axle (m); h is the height of vehicle center (m); and L is the wheelbase (m).

The f line group and r line group. The *f* line group is expressed as the ground braking force distribution curve of the front and rear axle, when the front wheels are locked but the rear wheels are not locked while braking on various φ values road. For the

f line group, the ground braking force relationship of front and rear axles is as follows

$$F_{br} = \frac{L - \varphi h}{\varphi h} F_{bf} - \frac{Gb}{h} \quad (2)$$

front wheels LOCKED and rear NOT

When the rear wheel is locked first than the front wheel while braking on various φ values, the braking force relationship of front and rear axles is r line group. For the r line group, the ground braking force relationship of front and rear axle is as follows

$$F_{br} = \frac{\varphi}{L + \varphi h}\left(Ga - hF_{bf}\right) \quad (3)$$

rear wheels LOCKED and front NOT

where φ is the ground adhesion coefficient; and a is the distance from the center of the mass to the center of the front axle (m).

ECE brake regulations. In order to ensure the braking stability of the vehicle, the rear wheel must have a certain braking strength when the front wheel is locked. To this end, the ECE developed the ECE-R13 brake regulations.[19] The ECE brake regulations set clear requirements for the front and rear axle braking forces of two-axle vehicle. When the braking strength $z = 0.2 \sim 0.8$, the adhesion coefficient curve of front axle should be above the adhesion coefficient curve of rear axle, so that the front wheel is first locked to ensure the directional stability of the vehicle when braking; the adhesion coefficient is satisfied to $\varphi \leq (z + 0.07)/0.85$, and close to the ideal curve ($\varphi = z$), in order to ensure a high adhesion utilization. For front-wheel drive vehicle, the ECE lower boundary line is

$$\begin{cases} F_{bf} = \frac{z + 0.07}{0.85} \cdot \frac{G(b + zh)}{L} \\ F_{br} = zG - F_{bf} \end{cases} \quad (4)$$

Only for FRONT WHEEL DRIVE VEHICLE

Braking force distribution of the front and rear axle

According to the relevant provisions of the ECE-R13 regulations, when the adhesion coefficient φ is between 0.2 and 0.8, the braking strength z should satisfy the relationship $z \geqslant 0.1 + 0.85(\varphi - 0.2)$ and φ_r should be below φ_f; when z is between 0.3 and 0.4, $\varphi_r \leq z + 0.05$, the braking forces of the front and rear axles of the vehicle should be distributed as equation (5).

$$\frac{\left(F_{br} + F_{bf}\right)^2 h}{GL} + \frac{b + 0.07h}{L}\left(F_{br} + F_{bf}\right) - 0.85F_{bf} + 0.07\frac{Gb}{L} = 0 \quad (5)$$

0.3<z<0.4

Make an ideal braking force distribution curve and an ECE regulatory curve according to equations (1) and (4), at the same time, equations (3) and (4) are substituted into the vehicle parameters and different values of pavement adhesion coefficient are taken for φ, the f and r line groups of the vehicle on the road surface with different adhesion coefficients are obtained. The braking force distribution

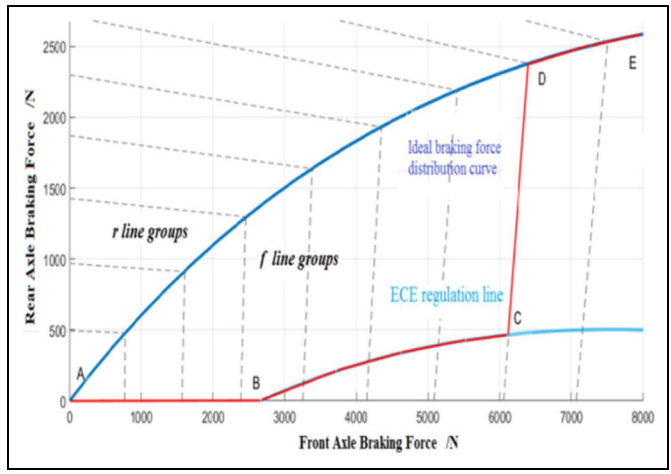

Figure 1. Braking force distribution characteristics of the front and rear axles.

characteristics of the front and rear axle of the vehicle can be obtained as shown in Figure 1.

It can be seen from Figure 1 that the coordinate value of point B is (2680, 0), and the corresponding braking strength is 0.21. When the braking strength is $0<z<0.21$, the braking performance of the vehicle is relatively reliable. The braking force is distributed according to the AB segment, and the braking force is all borne by the front axle to improve the energy recovery rate. At this time, the braking forces of the front and rear wheels are distributed as follows

$$\begin{cases} F_{bf} = zG \\ F_{br} = 0 \end{cases} \tag{6}$$

Based on the common adhesion coefficient of concrete and asphalt pavement 0.7, the intersection point C (6122, 467) between the *f* line and the ECE-R13 regulation line can be obtained, corresponding to a braking strength of 0.53. When the braking strength is $0.21<z<0.53$, in order to make the front axle bear the braking force as much as possible, the braking force of BC segment is distributed according to the M curve. At this time, the braking forces of the front and rear axles are distributed according to equation (2).

When the braking strength is $0.53<z<0.7$, the vehicle enters the emergency braking state easily. In order to ensure the stability of the braking performance and the braking energy recovery, the braking force is distributed according to the *f* curve of the CD segment $\varphi = 0.7$. At this time, the braking forces of the front and rear wheels are distributed as follows

$$\begin{cases} F_{bf} = \dfrac{zG}{K_{\mathrm{CD}} + 1} + \dfrac{K_{\mathrm{CD}} D_x - D_y}{K_{\mathrm{CD}} + 1} \\ F_{br} = zG - F_{bf} \end{cases} \tag{7}$$

where K_{CD} is the slope of line segment CD; D_x is the abscissa of point D; and D_y is the ordinate of point D.

When the braking strength is greater than 0.7, it is an emergency braking. In order to ensure the safety of the braking, at this time, the braking forces of the front and rear axle should be provided by a more reliable friction braking as much as possible, and distributed according to the ideal braking force distribution I curve of the DE segment, for braking distance. Then the braking forces of the front and rear axle are distributed as follows

$$\begin{cases} F_{bf} = \varphi G \dfrac{b + zh}{L} \\ F_{br} = \varphi G \dfrac{a - zh}{L} \end{cases} \tag{8}$$

Regenerative braking force analysis of the motor

The motor has four-quadrant operating characteristics, which can be converted into generator operation during braking. The characteristic curve of the generator approximates the characteristic curve of the motor. It can be concluded that the calculation model of the regenerative braking force of the motor is as shown in equation (9)

Regenerative braking force provided by the motor

$$F_e = \begin{cases} T_e i_1 \eta_T / r, 0 < n < n_N \\ 9550 P_N i_1 \eta_T / nr, n \geqslant n_N \end{cases} \tag{9}$$

where F_e is the regenerative braking force provided by the motor (N); T_e is the regenerative braking torque provided by the motor (N m); η_T is the transmission system efficiency; n_N is the rated speed of the motor (r/min); and n is the speed of the motor (r/min).

At the same time, in order to prevent the damage to the battery caused by excessive power generation, it is necessary to limit the output torque of the motor. The power generation can be calculated by equation (10) of the motor, the charging power of the battery can be obtained from equation (11), and the corrected torque of the motor can be obtained as equation (12)

$$P_{gen} = \frac{F_e r \omega \eta_T \eta_{gen}}{i_1} \tag{10}$$

power generation of the motor

$$P_{chg} = \left(E_b - I_{chg} R_b\right) I_{chg} \tag{11}$$

charging power of the battery

$$T_d = \frac{\min\{P_{chg}, P_{gen}\}}{\eta_{chg}\eta_{gen}\omega} \quad \text{Corrected torque of the motor} \tag{12}$$

where P_{gen} is the power generation of the motor (kW); ω is the angular velocity of the motor (rad/s); η_{gen} is the power generation efficiency of the motor; P_{chg} is the charging power of the battery (kW); E_b is the battery voltage (V); R_b is the internal resistance of the battery (Ω); I_{chg} is the charging current (A); η_{chg} is the charging efficiency; and T_d is the corrected torque of the motor (N m).

Simulation model of control strategy

Modeling of braking force distribution model

The relevant parameters of the vehicle, motor, and battery are shown in Table 1.

The braking performance required for different braking intents are different, and the braking forces assigned to the front and rear axles are also different. Based on automobile theory,[20] since the braking pressure is approximately linear with the brake pedal stroke, the brake pedal stroke percentage is taken as the braking strength in this article. According to equations (5)–(8), the braking force distribution model of the front and rear axle can be constructed in Simulink, which is shown in Figure 2.

Modeling of regenerative braking force distribution of the motor

According to the above analysis, it can be seen that the working characteristics of the motor and the battery are the key factors affecting the recovery of the braking energy.[21] In addition, the braking strength, the SOC signal of the battery, the vehicle

Table 1. Parameter table of the vehicle, motor and battery.

Parameter	Values
Full load quality of the vehicle (m/kg)	1250
Center of the mass height (h/m)	0.48
Wheelbase (L/m)	2.6
Distance from the center of the mass to the front axle center (a/m)	1.04
Windward area (A/m^2)	2.0
Wind resistance coefficient (C_D)	0.335
Rolling resistance coefficient (f)	0.09
Wheel radius (r/m)	0.31
Reduction ratio of the main reducer (i_1)	6.38
Rated power of the motor (P_N/kW)	75
Maximum speed of the motor (v/r/min)	10,000
Rated torque of the motor (T_N/N m)	240
Number of battery packs (n)	5
Maximum voltage of the battery pack (V^{-1})	420
Minimum voltage of the battery pack (V^{-1})	220

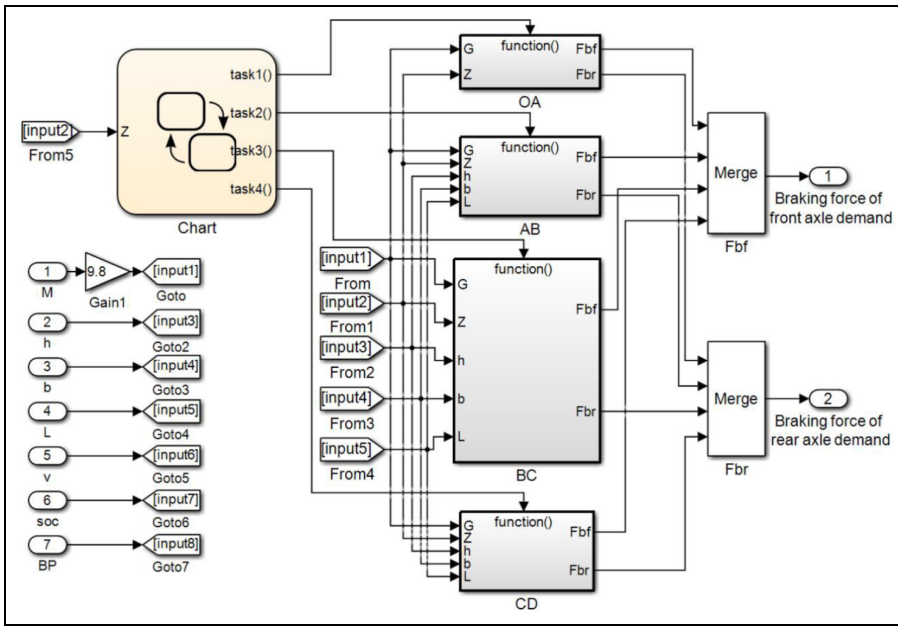

Figure 2. Braking force distribution model of the front and rear axle.

speed signal v, and the braking strength z are taken as inputs while using fuzzy control. The Mamdani type of controller is used, and the proportional coefficient K_e of the regenerative braking force of the motor to the front axle braking force are designed as the output signals, and the charging power characteristic of the battery is obtained to correct the output torque of the motor. Among them, the fuzzy subset of braking strength z is (low (L), medium (M), high (H)), the domain is [0, 1]; the fuzzy subset of vehicle speed v is (low (L), medium (M), high (H)), the domain is [0, 100]; the SOC fuzzy subset of the battery is (low (L), medium (M), high (H)), the domain is [0, 1]; the fuzzy subset of the regenerative braking proportional coefficient K_e is (very low (LL), low (L), medium (M), high (H), very high (HH)), the domain is [0, 1]; the membership functions of the braking strength z, the vehicle speed v, the battery SOC, and the regenerative braking proportional coefficient K_e are shown in Figure 3. The fuzzy control rules formulated are shown in Table 2, and the distribution model of the front axle braking force is shown in Figure 4).

Finally, the compilation tool is used to generate a ".dll" file of the entire Simulink model into the cruise simulation model.

Simulation results and analysis

According to the above strategy of braking force distribution, the road surface with an adhesion coefficient of 0.8 was selected for the simulation analysis of mild, moderate, and severe braking conditions in the co-simulation model.

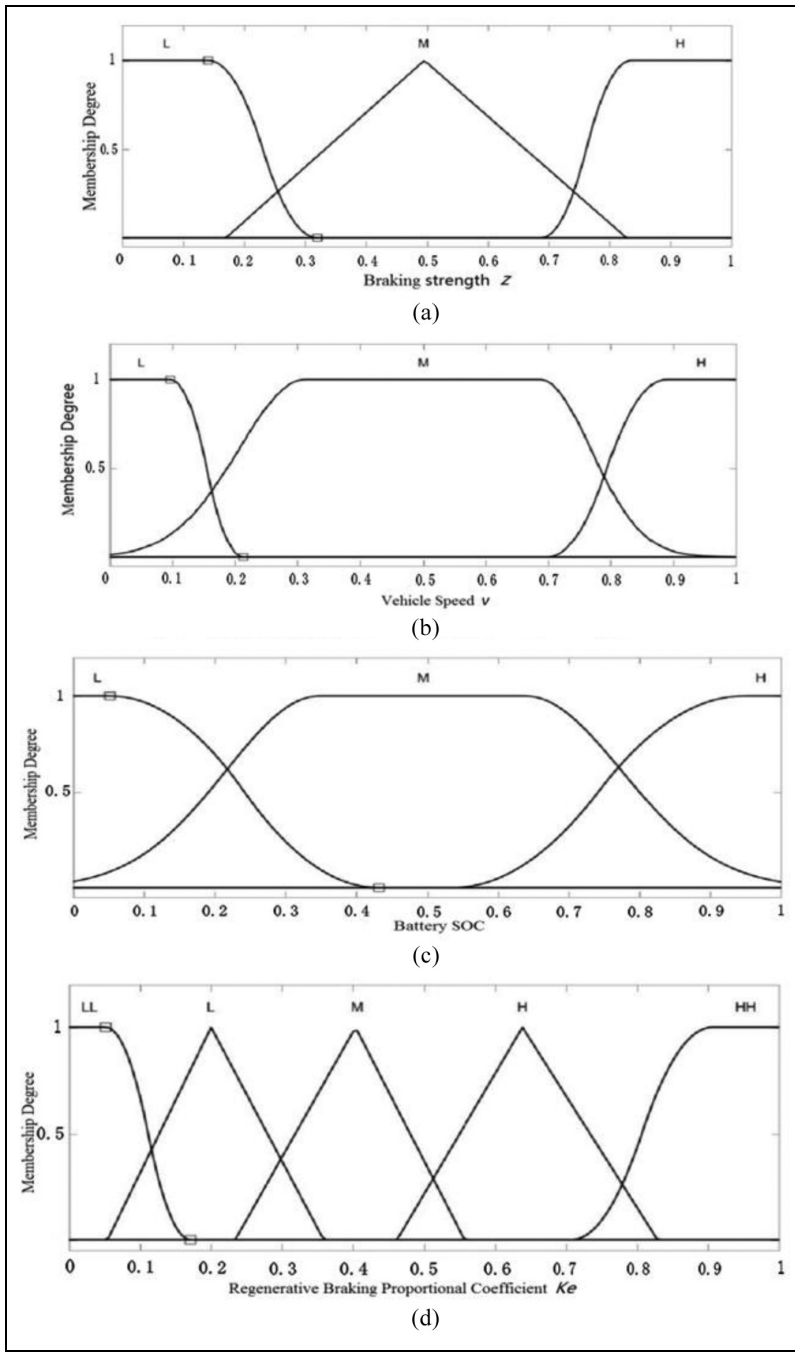

Figure 3. Membership function of input references: (a) membership function of the braking strength *z*; (b) membership function of the vehicle speed *v*; (c) membership function of the battery SOC; and (d) membership function of the regenerative braking proportional coefficient K_e.

Table 2. Fuzzy rule table of the regenerative braking ratio K_e.

Number	*v*	z	SOC	K_e
1	L	L	L	M
2	M	L	L	HH
3	H	L	L	HH
4	L	M	L	L
5	M	M	L	H
6	H	M	L	H
7	L	H	L	LL
8	M	H	L	LL
9	H	H	L	LL
10	L	L	M	M
11	M	L	M	HH
12	H	L	M	HH
13	L	M	M	L
14	M	M	M	H
15	H	M	M	M
16	L	H	M	LL
17	M	H	M	LL
18	H	H	M	LL
19	L	L	H	LL
20	M	L	H	LL
21	H	L	H	LL
22	L	M	H	LL
23	M	M	H	LL
24	H	M	H	LL
25	L	H	H	LL
26	M	H	H	LL
27	H	H	H	LL

SOC: state of charge; LL: very low; L: low; M: medium; H: high; HH: very high.

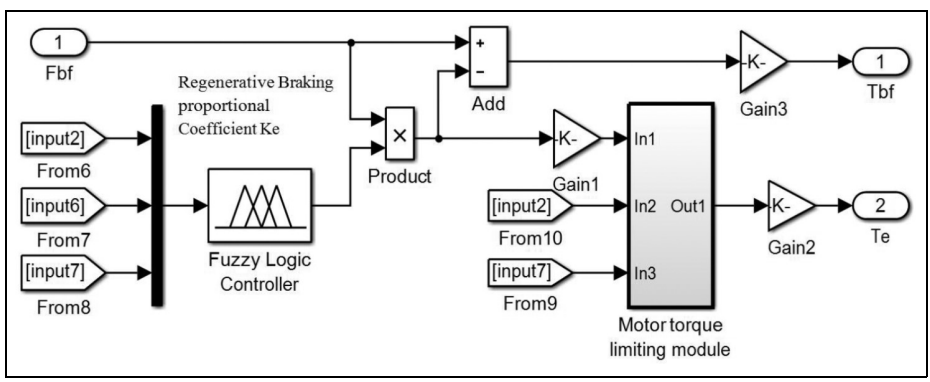

Figure 4. Braking force distribution model of the front axle.

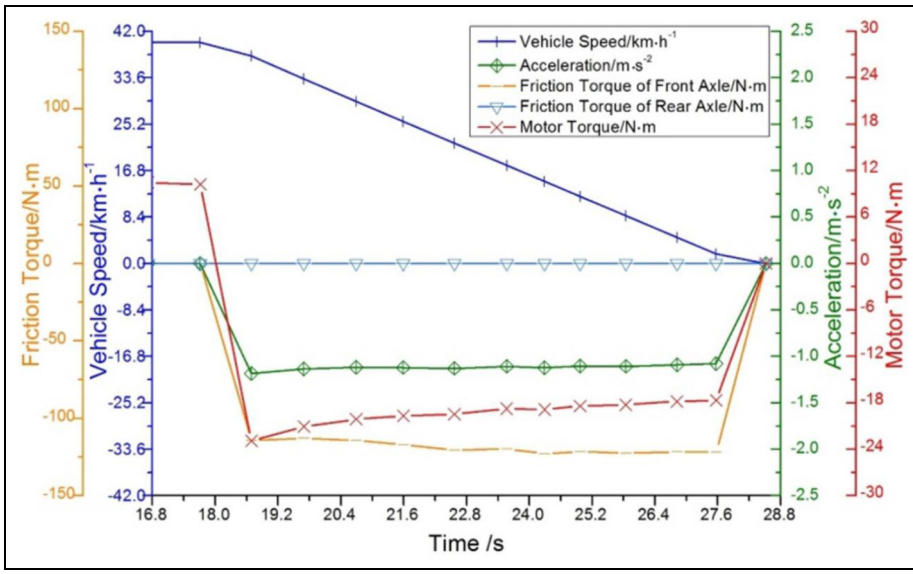

Figure 5. Braking force characteristics under mild braking conditions.

Analysis of braking force of the front and rear axle under different braking strengths

Mild braking condition. The setting of mild braking condition is shown in Figure 5. The initial speed is 40 km/h, the braking time is 10 s and the initial SOC is 74.78%. The friction torques of the front and rear axle and the output torque of the motor during the braking process of the vehicle are recorded, and the braking force characteristics under mild braking conditions are shown in Figure 5.

It can be seen from Figure 5 that the braking strength of this working condition is less than 0.21. The braking force is all provided by the front axle, the friction braking and regenerative braking work together, and the rear axle does not participate in the braking process, it complies with the braking force distribution rules of segment AB.

Moderate braking condition. The setting of the moderate braking condition is shown in Figure 6. The initial speed is 60 km/h, the braking time is 4 s, and the initial SOC is 74.61%.

It can be seen that the braking strength of this working condition is mostly between 0.21 and 0.53. The braking force is mainly borne by the front axle, and the proportion of the rear axle participation is relatively small. The braking force distribution of the front and rear axles is fitted to the BC section as shown in Figure 7. It is proved that the braking force distribution of this working condition is in accordance with the strategy formulated in this article. According to the fuzzy control rules of this article, the proportion of motor participation is larger.

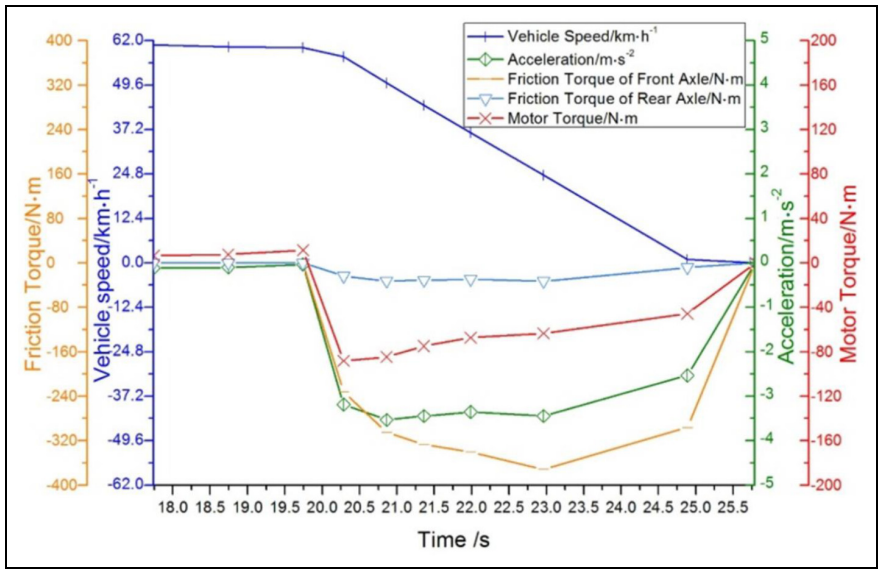

Figure 6. Braking force characteristics under moderate braking conditions.

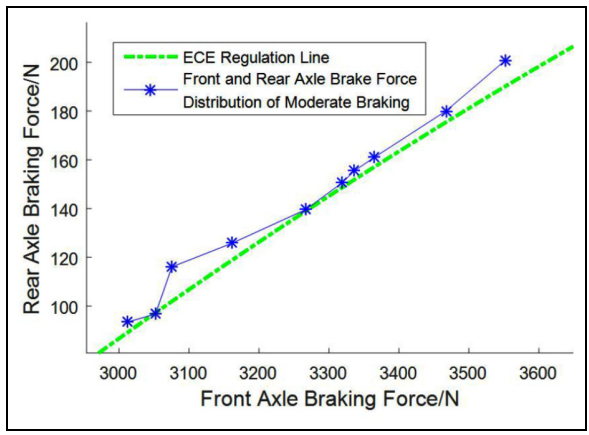

Figure 7. Braking force distribution of front and rear axles of moderate braking.

Severe braking condition. The setting of the severe braking condition is as shown in Figure 8. The initial speed is 90 km/h, the braking time is 4 s, and the initial SOC is 73.89%.

It can be seen that when the braking strength is between 0.53 and 0.7, in the case of high-speed braking, in order to ensure the braking stability and the energy

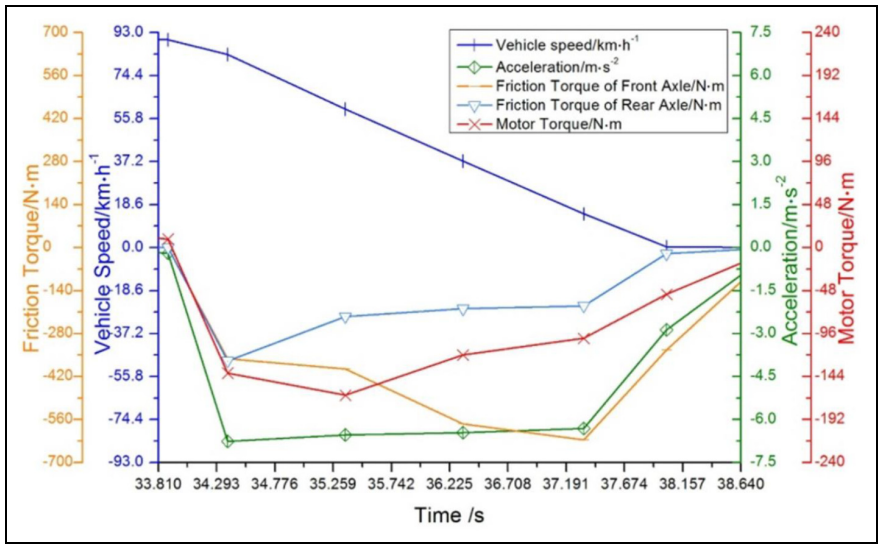

Figure 8. Braking force characteristics under severe braking conditions.

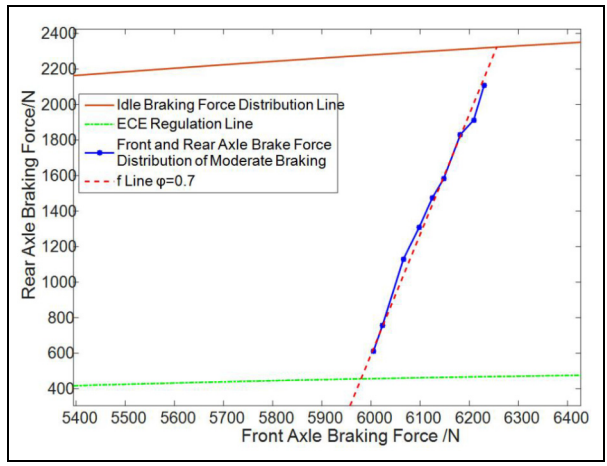

Figure 9. Braking force distribution of front and rear axles of severe braking.

recovery, the friction braking is the main factor, and the proportion of the motor participation decreases, at the same time, due to the influence of battery charging power, the growth of motor torque slows down, and the braking force distribution of the front and rear axles is fitted to the CD segment as shown in Figure 9, which is in accordance with the braking force distribution rule constructed in this article.

When the braking strength is greater than 0.7, it is emergency braking, according to the above braking force distribution rules, the motor hardly participates in

Table 3. Energy recovery of three braking conditions.

z	ΔE_k (kJ)	ΔE_c (kJ)	Recovery rate (%)	The SOC rise
$0<z<0.21$	77.15	21.13	27.39	0.03
$0.21<z<0.53$	173.68	75.44	43.43	0.11
$0.53<z<0.7$	390.63	164.04	42.01	0.25

SOC: state of charge; z: braking strength; ΔE_k: recyclable energy vehicle kinetic energy; ΔE_c: the energy recovered by the control strategy of this article.

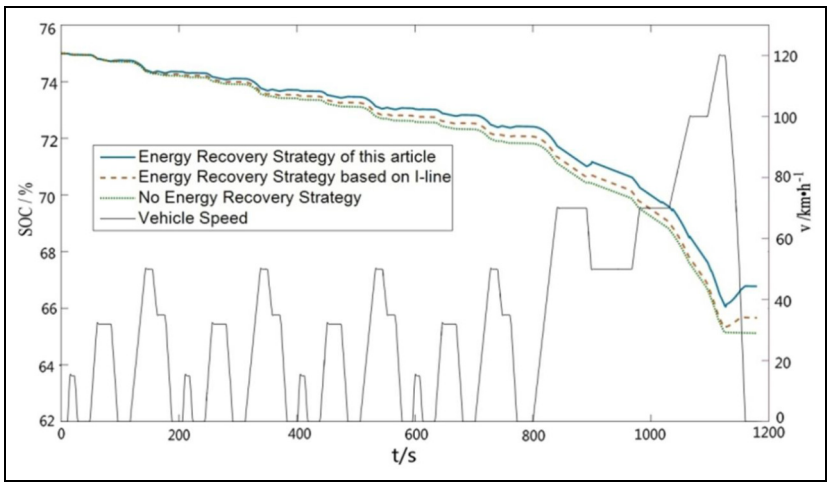

Figure 10. SOC curve with vehicle speed *v*.

braking and does not perform energy recovery. The energy recovery of the three braking strength conditions is shown in Table 3.

Battery SOC analysis under NEDC conditions

According to China's standard for the certification of electric vehicle cruising range, GB/T 18386-2017 "Test Method for Energy Consumption Rate and Cruising Range of Electric Vehicles," the braking energy recovery effect of this article is evaluated under NEDC conditions. The corresponding battery SOC curve with vehicle speed under different braking control strategies is shown in Figure 10.

It can be seen from Figure 10 that under the condition of initial SOC of 75%, the variation of SOC of braking control strategy in this article is the least, which is reduced by 8.22%, but the SOC of braking strategy based on I curve reduces by 9.12%, and the SOC reduces by 10% without braking energy recovery. The purpose of braking energy recovery is to improve the energy utilization rate of the

vehicle and extend the cruising range of the electric vehicle. Taking the using range of 95%–5% of battery SOC as calculation target, the cruising range of vehicle with braking control strategy of this article increases to 136.64 km. Compared with the braking strategy based on I curve, it increases by 10 km, and it increases by 22 km compared with the no braking energy recovery. It can be concluded that the braking control strategy of this article can effectively recover the braking energy.

Conclusion

1. A braking force distribution strategy of front and rear axle was proposed based on the I curve and ECE regulations of the braking characteristics of the vehicle. The distribution strategy of the regenerative braking force of the motor and friction braking force of the front axle was proposed and used the fuzzy control method, considering the working characteristics of the motor and battery.
2. A co-simulation model of the braking energy recovery control strategy of vehicle was proposed in Simulink and Cruise, according to the parameters of an electric vehicle model, and the control strategy proposed in this article was simulated under various braking conditions and NEDC conditions.
3. The results showed that the friction braking force of front and rear axle and the regenerative braking force of the motor were in accordance with the braking force distribution principle formulated in the article. The braking energy recovery rates under the three braking conditions were 27.39%, 43.43%, and 42.41%, respectively. Taking the using range of 95%–5% of battery SOC as calculation target, the cruising range of vehicle with braking control strategy of this article increases to 136.64 km. The braking energy recovery effect is valid, which could effectively improve the battery SOC and extend the cruising range.

Declaration of conflicting interests

The author(s) declared no potential conflicts of interest with respect to the research, authorship, and/or publication of this article.

Funding

The author(s) disclosed receipt of the following financial support for the research, authorship, and/or publication of this article: This research was supported under National Nature Science Foundation of China (51205055), Science and Technology Major Project in Heilongjiang Province (E2016003), and the Fundamental Research Funds for the Central Universities (2572019BG01).

ORCID iD

Shengqin Li https://orcid.org/0000-0002-4400-6872

References

1. Zhang JL, v C, Li Y, et al. Development status and prospect of brake energy recovery technology for electric drive passenger cars. *Automot Eng* 2014(8): 911–918.
2. Chu L, Cai J, Fu Z, et al. Research on brake energy regeneration evaluation and text method of pure electric vehicle. *J Huazhong Univ Sci Technol* 2014(1): 18–22.
3. Oliveira ADM, Bertoti E, Eckert JJ, et al. Evaluation of energy recovery potential through regenerative braking for a hybrid electric vehicle in a real urban drive scenario. SAE technical papers 2016-36-0348, 2016.
4. Wang M, Sun Z, Zhuo G, et al. Braking energy recovery system for electric vehicle. *Trans Chin Soc Agri Mach* 2012; 43(2): 6–10.
5. Aimo BM, Colombano M, Imarisio M, et al. Braking method and device with energy recovery in particular for a vehicle equipped with hybrid traction system. Patent US8137235B2, 2012.
6. Cornic D. Efficient recovery of braking energy through a reversible dc substation. In: *Proceedings of the electrical systems for aircraft, railway and ship propulsion*, Bologna, 1–21 October 2010, pp. 1–9. New York: IEEE.
7. Wang Q, Qu X, Yu Y, et al. A study on the power allocation strategy for hybrid electric bus with compound electric powers. *Automot Eng* 2014; 36(4): 389–393.
8. Ruan J and Walker P. An optimal regenerative braking energy recovery system for two-speed dual clutch transmission-based electric vehicles. SAE technical paper 2014-01-1740, 2014.
9. Wang M, Sun Z, Zhuo G, et al. Maximum braking energy recovery of electric vehicles and its influencing factors. *J Tongji Univ* 2012; 40(4): 583–588.
10. Ko JW, Ko SY, Kim IS, et al. Co-operative control for regenerative braking and friction braking to increase energy recovery without wheel lock. *Int J Automot Tech* 2014; 15(2): 253–262.
11. Zhang L, Wang G, Zhang Y, et al. ABS control performance of integrated brake system with regenerative friction brake in electric vehicle. *Trans Chin Soc Agri Mach* 2015; 46(10): 350–356.
12. Yang Y, Zou J, Yang Y, et al. Pressure coordinated control system for HEV regenerative braking. *J Mech Eng* 2014; 50(22): 127–135.
13. Montazeri-Gh M and Mahmoodi-K M. An optimal energy management development for various configuration of plug-in and hybrid electric vehicle. *J Central South Univ* 2015; 22(5): 1737–1747.
14. Gao Y and Ehsani M. Design and control methodology of plug-in hybrid electric vehicles. *IEEE T Ind Electron* 2010; 57(2): 633–640.
15. Gao H, Chu L, Guo J, et al. Control strategy of braking energy recovery based on electric servo system. *Trans Chin Soc Agri Mach* 2017; 48(7): 345–352.
16. Hu M, Chen S and Zeng J. Coordinated control for mode-shift of dual-motor coupling powertrain. *J Mech Eng* 2017; 53(14): 73–81.
17. Chen Z, Tan G, Lin C, et al. Braking energy recovery of pure electric vehicle based on fuzzy algorithm. *J Guangxi Univ Sci Technol* 2014; 25(3): 32–37.
18. Meng T. *Research on control strategy of regenerative braking system of electric vehicle based on driving cycle*. Master Thesis. Hefei University of Technology, Hefei, China, 2017.
19. ECE Regulation No.13 Rev.8, Uniform provisions concerning the approval of vehicles of categories M, N and O with regard to braking.

20. Yu Z. *Automobile Theory*. 5th ed. Beijing: Mechanical Industry Press, 2015.
21. Gong X, Zhang L, Ma J, et al. Braking force distribution of electric vehicle based on braking stability requirements. *J Chang'an Univ* 2014; 34(1): 103–108.

Author biographies

Shengqin Li, Ph.D., is an Associate Professor, whose research interests is vehicle dynamics and control.

Bo Yu, Master, whose research interests is electric vehicle power train control.

Xinyuan Feng, Master, whose research interests is vehicle dynamics and control.